**Proceedings of the ASME 2020 15th International Manufacturing Science and Engineering Conference**
**MSEC2020**
**June 22-26, 2020, Cincinnati, OH, USA**

**MSEC2020-8388**

# REDUCING VARIABILITY IN CHEMICAL VAPOR DEPOSITION OF CARBON NANOTUBES BASED ON GAS PURIFICATION AND SAMPLE SUPPORT REDESIGN

**Golnaz Tomaraei**
Department of Industrial Engineering
University of Pittsburgh
Pittsburgh, PA, USA

**Moataz Abdulhafez**
Department of Industrial Engineering
University of Pittsburgh
Pittsburgh, PA, USA

**Jaegeun Lee**
Department of Organic Material Science and Engineering, Pusan National University
Department of Industrial Engineering
University of Pittsburgh
Pittsburgh, PA, USA

**Mostafa Bedewy***
Department of Industrial Engineering, Department of Chemical and Petroleum Engineering, Department of Mechanical Engineering and Materials Science
University of Pittsburgh, Pittsburgh, PA, USA
*mbedewy@pitt.edu

## ABSTRACT

The synthesis of vertically aligned carbon nanotubes (CNTs), also referred to as CNT forest, by chemical vapor deposition (CVD) is an intricate process that is sensitive to multiple factors other than control of temperature, pressure, and gas flows. In particular, growth is highly sensitive to factors like ambient humidity, as well as small quantities of oxygen-containing species and carbon deposits inside the reactor. These typically uncontrolled factors significantly affect growth reproducibility and hinders the fundamental study of process-structure-property relationship for these emerging materials. Accordingly, universally applicable design modifications and process steps toward improve growth consistency are sought after. In this study, we introduce two new modifications to our custom-designed multizone rapid thermal CVD reactor and demonstrate their impact on growth: (1) reconfiguring the inlet gas plumbing to add a gas purifier to the helium (He) line, and (2) designing a new support wafer for consistent loading of substrates. We use statistical analysis to test the effectiveness of these modifications in improving growth and reducing variability of both CNT forest height and density. Analysis of our experimental results and hypothesis testing show that combining the implementation of He purifier with the redesigned support wafer increases forest height and reduces the variability in height (17-folds), both at statistically significant and practically significant levels.

## 1. INTRODUCTION

A vertically aligned CNT forest is composed of tens to hundreds of billions of CNTs per $cm^2$ which interact to self-orient during the early growth stages and to maintain the aligned forest morphology of mechanically coupled CNTs until several-millimeters height is achieved [1–4]. The resulting highly anisotropic structure together with the outstanding properties of individual CNTs make these forests promising candidates for various applications, including thermal interfaces [5], separation membranes [6], and electrical interconnects [7]. Understanding the bulk properties of these forests requires obtaining representative statistical information from individual nanotubes [2]. A statistical approach can also used to optimize experiment design by identifying the most influential parameters. For example, Pander *et al.* used Taguchi method to dramatically decrease the number of annealing experiments required to control and reduce the size and roughness of catalyst nanoparticles [8]. In spite of all these improvements, further research is still required to resolve the problem of run-to-run variation (consistency issue) in CNT forest growth.

Although CNT forests are promising for many applications, one of the main challenges in their scalable production by CVD is reproducibility, which limits fundamental studies on growth and deactivation mechanisms as well as properties optimization. Due to the importance of establishing robust synthesis processes, the inconsistency issue has been previously studied by multiple research groups. Noy *et al.* showed that trace amount of water vapor (~ 1 ppm) can have a significant effect on growth kinetics

 

[9, 10]. They mention that extremely tight control of the reaction gas composition purity is necessary to obtain controlled growth of CNTs under atmospheric CVD conditions. Hart *et al.* performed statistical analysis on 280 samples and showed the effect of ambient humidity on the variability of growth [11], and demonstrated the use of reactor with dynamic arm to mitigate moisture transience for improving growth consistency [12]. Plata *et al* showed that different concentrations of oxygen lead to different growth behaviors. They pointed out that low concentrations of oxygen can boost Ostwald ripening of Fe catalyst nanoparticles, which can be reduced by $H_2$ [13]. Carpena-Núñez *et al.* [14] and Dee *et al.*[15] showed that trace carbon residues on reactor walls influence the growth as well. Therefore, some universally applicable processing steps are required to reduce the adverse impact of uncontrolled quantities of chemical species on the consistency of CNT forest growth. In this regard, various processing steps such as pumping [16, 17], cycled pumping [18], and heating of gas line with pumping [19] have been introduced prior to growth.

Previous work from our group has shown that pumping with mild baking at 200 °C prior to catalyst formation resulted in a significantly improved process consistency by reducing the coefficient of variation of forest heights (by a factor of 6) [20]. The use of coefficient of variation as a statistical measure of consistency allowed comparing different means of populations and proved to be an effective measure under the different procedures used in the study. In our process, we also do a 1000°C bake between growth experiments to reduce the influence of carbon residues in the reactor.

In continuation of efforts to improve process reproducibility, we explore the influence of two aspects not previously addressed in previous work: (1) cylinder-to-cylinder variations of background gas (He), and (2) substrate support design for positioning and temperature uniformity across the sample. Due to the sensitivity of the process to oxygen containing species at the ppm level, slight variations of contaminants between He cylinders (the background gas in our reactor) affect process consistency in an uncontrolled fashion. Additionally, due to the IR heating nature of our cold wall reactor, sample temperature non-uniformity arises from geometric and emissivity variations [21], which are dictated by substrate support and precise positioning of the sample from one experiment to another. Here, we develop approaches to reduce and control these effects. To alleviate the effect of cylinder-to-cylinder variations, we add a gas purifier to the He line in our custom-built reactor to reduce the stochastic effects of oxygen-containing contaminants. To improve temperature uniformity, effect of chip size and positional stability of the catalyst chip in the reactor, we design an improved sample support. We use statistical hypothesis testing to assess the efficacy of these modifications and show that these universally applicable approaches can improve process reproducibility and consistency if adopted in other reactors.

## 2. MATERIALS AND METHODS

### 2.1 Sample preparation

Si (001) with a 300-nm thick $SiO_2$ layer was first coated with a 10 nm thick alumina layer using atomic layer deposition (ALD) technique. Then, E-beam evaporation was used to deposit a 1-nm thick Fe catalyst layer on top of alumina support layer. Samples of approximately 5 mm × 5 mm were cut from the catalyst-coated substrate and were loaded into our custom-designed multizone rapid thermal CVD reactor (Figure 1).

### 2.2 CNT forest growth

In this reactor, gas-phase hydrocarbon molecules are thermally decomposed within a resistive preheater, which is next to an IR heater where both catalyst treatment and CNT growth take place [22, 23]. Due to the poor absorptivity of gases to IR radiation as well as their short residence time around the heated substrate compared to their residence time inside the preheater, the possibility of gas phase reactions within the IR reactor is negligible. Additionally, the chance of recombination of the pre-decomposed gas is minimized owing to the short traveling distance from the preheater to the substrate. The rapid thermal processing (RTP) capability of the IR heater, which enables fast heating of the substrate with rates greater than 50 °C/min, together with high cooling rates due to the relatively low thermal mass allow the decoupling of catalyst formation and CNT growth steps [23].

Figure 2a and 2b show an example of decoupled and coupled recipes, respectively. It is worth noting that in a decoupled recipe, the growth temperature ($T_g$) and the catalyst formation temperature ($T_c$) can be equal, but there is a cooling and reheating step between catalyst formation and growth steps. Therefore, decoupled recipes are generally more sensitive to small variation in other growth conditions, possibly due to longer exposure of catalyst particles prior to growth [20]. Therefore, coupled or semicoupled recipes, wherein temperatures go directly from $T_c$ to $T_g$ without cooling down first, are more consistent for fundamental studies of growth. The growth recipes are explained in detail elsewhere [23]. Figure 2-c shows a several-mm CNT forest grown within our reactor. SEM images at low and high magnifications, Figure 2-d and 2-e respectively, show the alignment of nanotubes in a vertically aligned CNT (VACNT) forest.

 

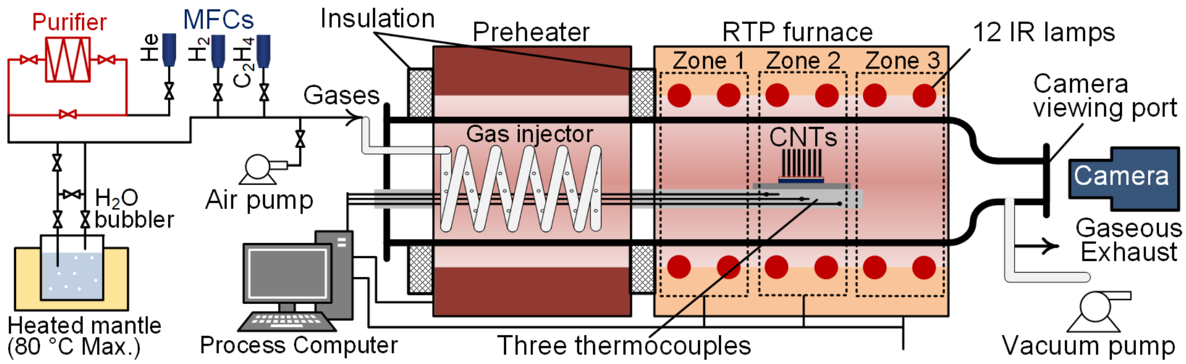


**Figure 1:** Schematic illustration of the custom-designed multizone RTP CVD reactor used in this study showing the added He purifier

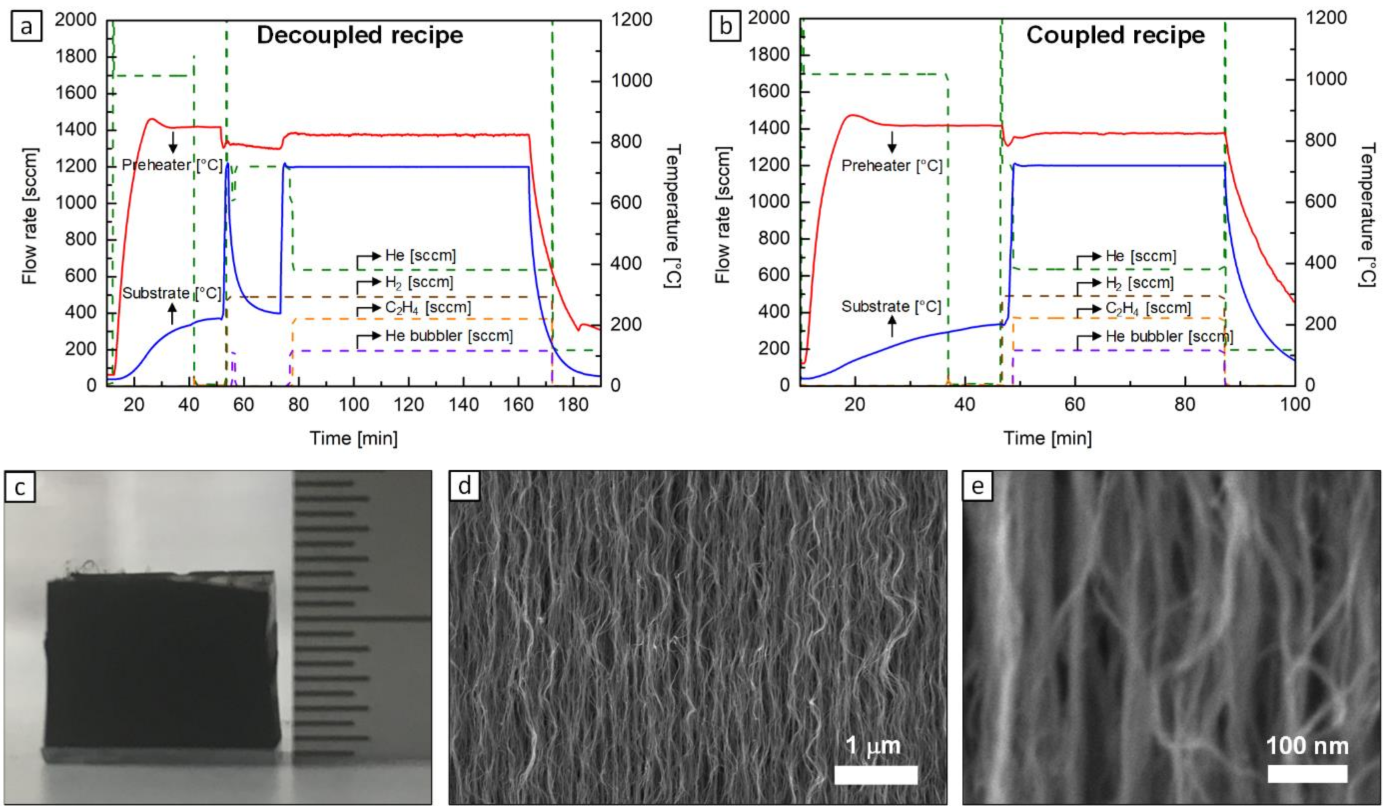


**Figure 2:** Typical (a) decoupled and (b) coupled recipes used for CNT growth in our RTP CVD reactor. (c) optical image of several-millimeter high CNT forest grown in reactor. SEM images at (d) low and (e) high magnifications showing the alignment of individual CNTs within the forest.

### 2.3 Height and density measurement of CNT forests

For accurate measurements of the height and volume of each CNT forest, a 3D optical microscope (VR-3000 series, Keyence) was utilized to get a digital imprint of forest geometry. CNT forest mass was measured using sensitive balance before and after growth. Knowing the mass of the CNT, the volumetric density of each CNT forest was calculated. Moreover, scanning electron microscopy (SEM) imaging was done using a Zeiss SIGMA VP Microscope.

## 3. RESULTS AND DISCUSSION

### 3.1. Effect of changing He cylinder on growth

Any fundamental study on CNT forest growth requires running a large number of experiments and therefore involves changing gas cylinders regularly, especially the He gas, which is consumed the most. Unknown effects of changing cylinder on growth therefore adds to the uncertainty of results from these studies and may render them unreliable. Since He cylinder is the most frequently changed cylinder, here we first investigate the effect of He cylinder change on CNT forest height. A decoupled growth recipe with $T_c$ = 720 °C and $T_g$ = 720 °C was used with five sample sets, each containing at least six forests. As listed in Table 1, pumping time prior to IR heating varied between 0, 10, and 20 minutes. Here, μ refers to mean height, σ refers to standard deviation, and CV refers to the coefficient of variation.

**Table 1:** Statistical analysis of height obtained from CNT forests grown under the described recipes using three different He cylinders

| Sample | Recipe | μ | σ | CV | Sample size | He cylinder |
|---|---|---|---|---|---|---|
| 1 | Decoupled, He-rich annealing, No-pumping, hot-open | 0.897 | 0.479 | 0.534 | 6 | 1 |
| 2 | Decoupled, He-rich annealing, No-pumping, cold-open | 0.721 | 0.225 | 0.311 | 7 | 2 |
| 3 | Decoupled, He-rich annealing, 10 min-pumping, cold-open | 1.249 | 0.106 | 0.085 | 6 | 1 |
| 4 | Decoupled, He-rich annealing, 20-min pumping, hot-open | 0.804 | 0.089 | 0.111 | 7 | 2 |
| 5 | Decoupled, He-rich annealing, 20-min pumping, cold open | 0.921 | 0.156 | 0.169 | 7 | 3 |

In all experiments, we avoid opening the reactor until the temperature drops below 200 °C. The reasons are to minimize the likelihood of adsorption of gaseous species on the walls of the reactor, and also to avoid exposing CNTs to air unless their temperature is low enough to avoid oxidation or degradation of CNTs. Cold-open refers to the cases in which enough wait time for cooling was allowed after baking to reach temperatures in the range of 30-80 °C before opening the reactor to load the sample, while hot-open refers to the cases in which the temperature was in the range of 130-200 °C when opening the reactor. These slight differences in processing parameters should not have a considerable effect on the variability of forest growth based on the previous study of our group [20].

Figure 3 shows that vacuum baking prior to IR heating improves the variability in the height of the forests. It also shows that changing He cylinder could affect the height of the forests. This is the reason why we focused on coefficient of variation (CV) when comparing different populations of CNT forests grown according to different conditions, in our previous work [20]. Another limitation of that previous study is that it focused on height measurements only and did not study the variability in the density of the forests.

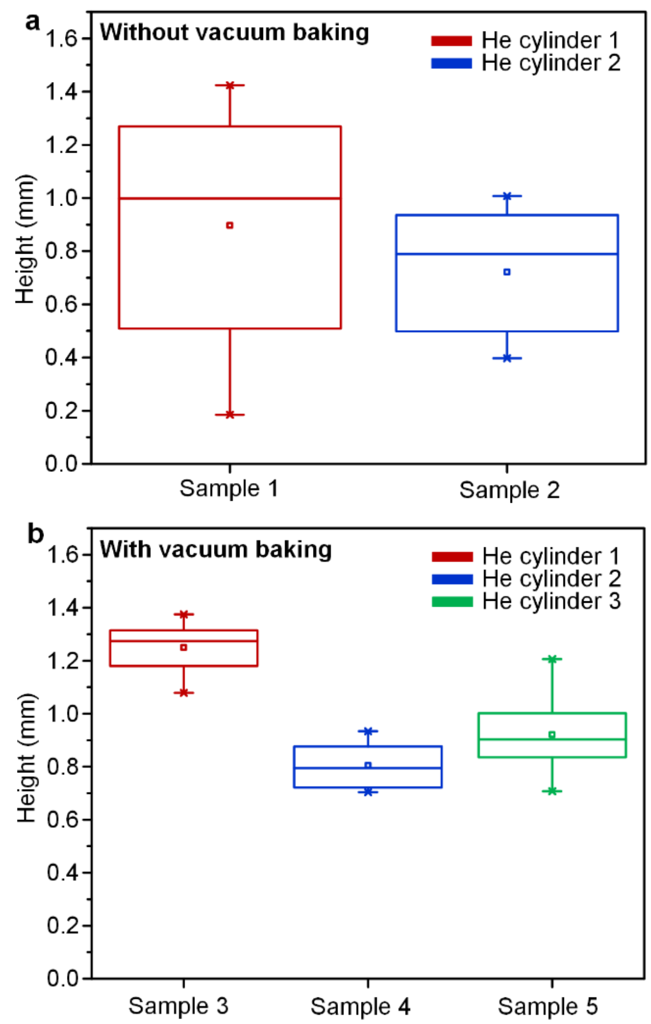


**Figure 3:** Box plots for height measurements of CNT forests belonging to five different sample populations detailed in Table 1, which were all grown according to the same growth recipe. (a) without vacuum baking and (b) with vacuum baking prior to IR heating

To further study the effect of changing He cylinder on both height and density of CNT forests, two sample sets of experiments, each containing five forests, were prepared according to the same recipe (coupled recipe with $T_c$ = 650 °C and $T_g$ = 650 °C) using two different He cylinders (referred to here as cylinders 4 and 5). The results of statistical analysis of t-test presented in Table 2 and Figure 4 reveal that the average densities are different at a significance level of 0.05.

**Table 2:** Statistical analysis of height and density of two samples of five CNT forests grown using two different He cylinders

| He Cylinder | Height (mm) | | | T test | | Sample size |
|---|---|---|---|---|---|---|
| | μ | σ | CV | Statistic | p-value | |
| 4 | 1.072 | 0.139 | 0.130 | 1.106 | 0.301 | 5 |
| 5 | 0.991 | 0.088 | 0.089 | | | 5 |
| He Cylinder | Density (g/cm$^3$) | | | T test | | Sample size |
| | μ | σ | CV | Statistic | p-value | |
| 4 | 0.015 | 0.002 | 0.157 | -2.532 | 0.035 | 5 |
| 5 | 0.019 | 0.003 | 0.139 | | | 5 |

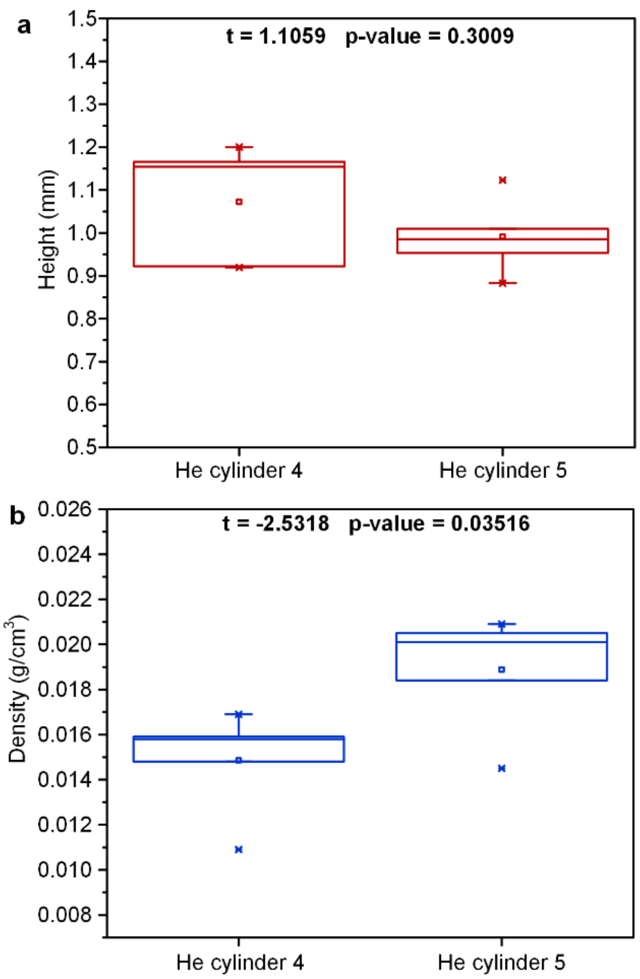


**Figure 4:** Box plots for CNT forest (a) height and (b) density using the same growth recipe with two different He cylinders

Hence, Figures 3 and 4 together show that changing He cylinder can significantly influence the growth results. One possible explanation is that the variation in the level of purity of the gas from one cylinder to another leads to small variations of water vapor level or oxygen level. This is consistent with the findings of other researchers who reported the small quantities of chemical species, especially oxygen-containing molecules, with uncontrolled concentrations inside the reactor as the main cause of variability in growth. Although we also observe some dependence of variability on the recipe (i.e. coupled vs. decoupled), our goal is to develop our process in such a way that it reduces the problem of run-to-run variation for all recipes. Therefore, we next focused on reducing the level of gas impurity and its effect on growth consistency.

### 3.2. New modifications to address variability problems

We modified two things in our growth setup. We installed a purifier for the He gas line, as shown in the top left corner of Figure 1. We also designed a new support for the substrate, as shown in Figure 5. In our IR-heated zones, using a support wafer in contact with the substrate eliminates the movement of the substrate and reduces temperature variability. With the new design, there is less possibility of creating a gap between substrate and support, which in turn creates a more uniform temperature profile across the substrate.

#### 3.2.1 Installing He purifier

While we use ultra-high purity grade He cylinders (99.999%) with contaminants level in the range of ppm, to further remove uncontrolled gas impurities, we installed a purifier (Entegris, model MC190-902F) between He cylinder and its mass flow controller. It is capable of reducing $H_2O$, $O_2$, CO, $CO_2$, and $H_2$ impurities to less than 100 part per trillion (ppt). There are very few techniques with the ability to detect these small quantities of contaminants. Additionally, most of the available techniques cannot distinguish among different contaminants. The main challenge we are resolving in our work is that growth is very sensitive to small quantities of gaseous species that are difficult to measure or control. One goal of our work is therefore to develop the process to be more consistent even if we don't know what the contaminants are. As the schematic of our custom-designed reactor in Figure 1 shows, the purifier is integrated into the system with a bypass capability that enables us to compare growth experiments run with and without this purifier.

#### 3.2.2 New substrate support design

For the baseline process, we used two pieces cut from a 3" silicon wafer around the catalyst-coated chip, as shown in Figure 5b, to fix its position and to improve its temperature uniformity during growth. With this design, catalyst-coated Si chips used to move by tens of millimeters as they were free to slide on the quartz holder. In the new support design, a full 2" wafer is used instead with a microfabricated central recessed area to fit catalyst-coated Si chips, as shown in Figure 5c. The chips are therefore confined within the recessed geometry of the support and can only move within the clearance in the range of ≈100 µm. Also, the new support itself is placed in the same location on the quartz holder every time, as marked by the flat edges of the geometry. Since the support wafer doesn't move during growth, we estimate that its placement is within one millimeter from growth to growth. Hence, the new support design eliminates two separate issues with positioning the samples in the old design, which have been causing variability of results. This design also improves temperature uniformity across the catalyst. To fabricate the new support wafer, we use a 2" silicon wafer with native oxide layer. The fabrication process is described in Figure 5-a. We spin coat the wafer with a layer of positive lift-off resist (LOR) and a layer of positive photoresist (PR). We then use a maskless aligner (MLA) to expose the entire wafer except for a 10 × 10 mm$^2$ square pattern in its center. The wafer is then developed to remove the exposed LOR and PR. A 100 nm layer of chromium is then deposited using e-beam deposition as a hard-etching mask. Lift off is then carried out using sonication in a PR solvent, followed by reactive ion etching (RIE) using sulfur hexafluoride as an etching gas for 30 minutes. Following the etching, the Chromium is removed using Chromium etchant. The resulting wafer has a 10 × 10 mm square recess that is around 50 µm in depth. The recessed area in this design is sized to fit the catalyst-coated chips used in the study. Figure 5d shows the profilometry data across the edge of the groove, illustrating the depth of the groove.

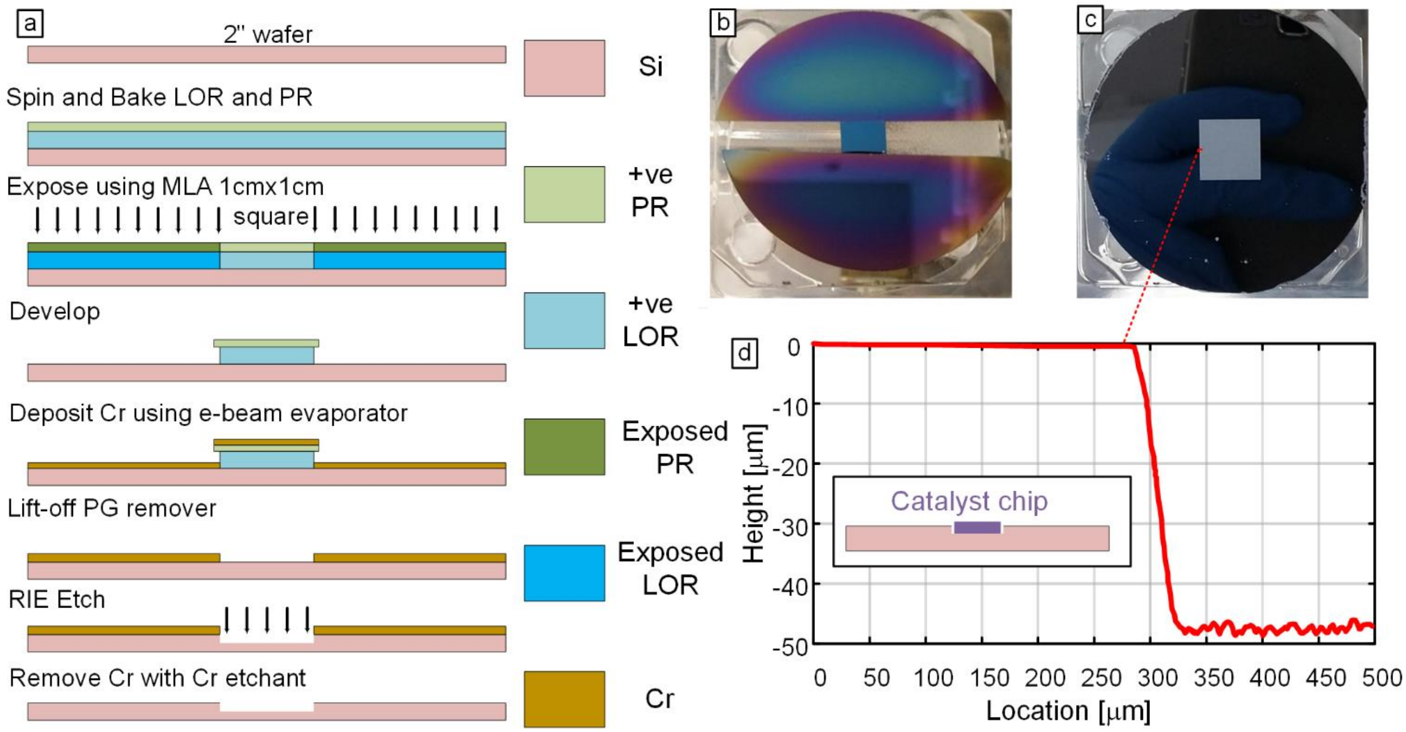


**Figure 5:** Schematic of the fabrication process for the new support, (b) The support wafer used for baseline growth process consists of two pieces cut from a 3" silicon wafer, (c) the new microfabricated 2" support wafer with designed recess to fit the substrate. (d) Profilometry across the edge of the recess at the center of the new support shows that its depth is ≈50 µm.

### 3.3. Effect of He purifier and new substrate support

We studied the combined effect of the two modifications that we made to our growth setup. A coupled growth recipe with $T_c$ = 700 °C and $T_g$ = 700 °C was used for all forest growth experiments in this section. Each sample set consisted of at least 5 forests. In the baseline setup, the support wafer in Figure 5b was used and He flow bypassed the purifier. In the setup with He purifier, the support wafer in Figure 5b was used and He flow through the purifier was allowed. In the setup with He purifier + new support, the support wafer in Figure 5c was used and He flow through the purifier was allowed. Figure 6 shows that using He purifier and the new support wafer together increased the height and density of the forests. The diameter of CNTs, however, is more dependent on the thickness of the deposited catalyst films and slightly dependent on temperatures of catalyst formation and CNT growth. While it can change based on the growth recipe, as reported in our previous work [23], in the present study we don't expect diameters to change since we are only repeating the same recipe with the presence of He purifier and with the redesigned support wafer.

 

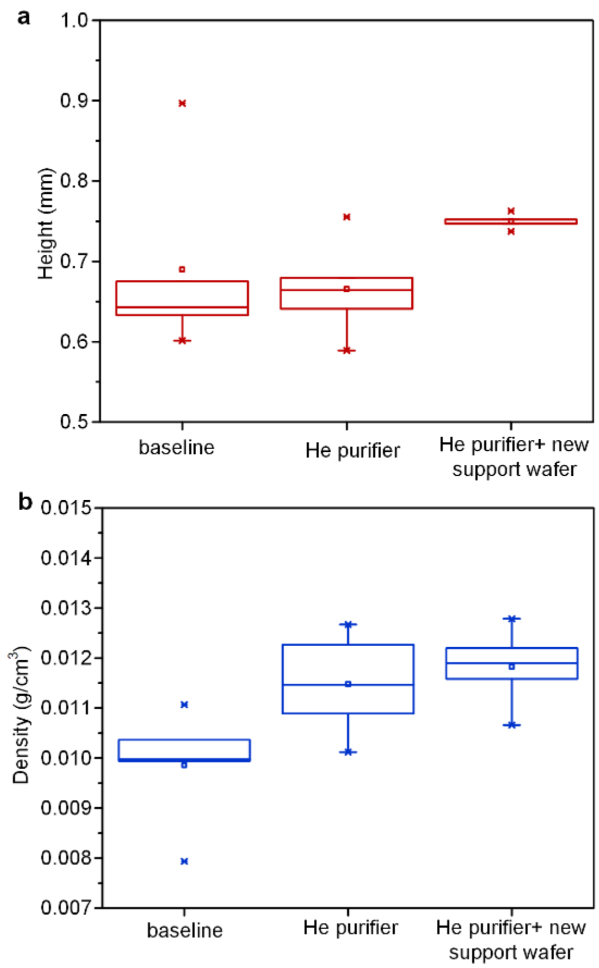


**Figure 6:** Box plots for CNT forest (a) height and (b) density using the same growth recipe with three different growth setups

To investigate whether the change in height and density of the forests as a result of introducing He purifier and new support wafer is statistically significant, we used t-test for testing the hypotheses concerning the equality of height and density for different pairs of sample populations grown according to three cases described above and in Tables 3 and 4. As listed in Table 3, when He purifier is installed, the change in the height as a result of changing the support wafer is statistically significant.

Additionally, CV is calculated for the height and density of the forests as a measure of relative variability. The results in Figure 7 show that CV decreases when He purifier and the new support wafer are used. A 17-fold decrease of CV of heights was observed, and a 2-fold decrease of CV of densities was observed. Nevertheless, to examine whether the effect of the two modifications on the CV of forest height and density is statistically significant or not, we used the cvequality package [24] in R software to test statistical hypotheses concerning the equality of CV for different pairs of growth setups shown in Table 5.

**Table 3:** Results of statistical tests for equality of the height of CNT forests. The same recipe with and without He purifier and with two different support wafers (Figure 5b and c). P-values less than 0.05 are marked bold.

| Growth process | T test | |
|---|---|---|
| | Statistic | p-value |
| Baseline vs He purifier | 0.453 | 0.661 |
| He purifier vs He purifier + new support | 3.738 | **0.0134** |
| Baseline vs He purifier + new support | 1.132 | 0.3206 |

**Table 4:** Results of statistical tests for equality of the density of CNT forests. The same recipe with and without He purifier and with two different support wafers (Figure 5-b and c). P-values less than 0.05 are marked bold.

| Growth process | T test | |
|---|---|---|
| | Statistic | p-value |
| Baseline vs He purifier | 2.556 | **0.0308** |
| He purifier vs He purifier + new support | 0.6528 | 0.5302 |
| Baseline vs He purifier + new support | 3.129 | **0.014** |

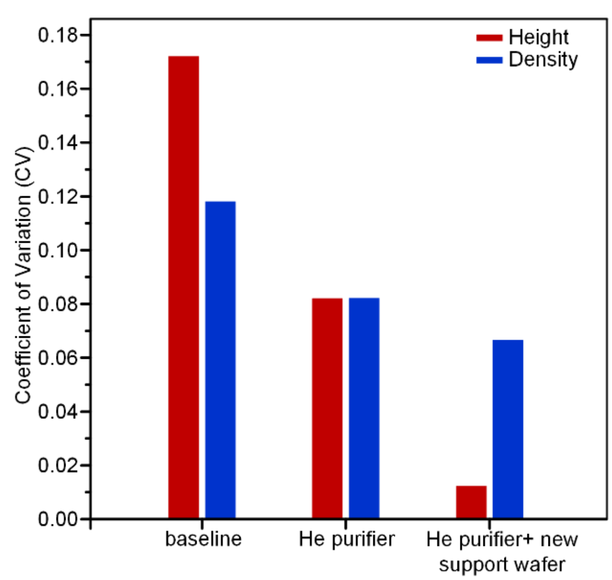


**Figure 7:** The effect of the modifications to the growth process on reducing the coefficient of variation in height and density of CNT forests. The same growth recipe was used in all cases (coupled growth at $T_c$ = 700 °C and $T_g$ = 700 °C)

We used two statistical tests to compute test statistics and p-values: asymptotic test by Feltz and Miller [25] as well as modified signed-likelihood ratio test (M-SLRT) by Krishnamoorthy and Lee [26]. More details about the statistical hypotheses can be found elsewhere [20]. Test statistics and p-values listed in Table 5 reveal that adding He purifier along with using the new support wafer (Figure 5c) led to a statistically significant change in the CV of forest height. However, the change in the CV of forest density between the studied pairs was not statistically significant.

**Table 5:** Results of statistical tests for equality of CV of CNT forest height and density. The same recipe with and without He purifier and with two different support wafers (Figure 5-b and c). P-values less than 0.05 are marked bold.

| Height | | | | |
|---|---|---|---|---|
| | asymptotic | | M-SLRT | |
| | statistic | p-value | statistic | p-value |
| Baseline vs He purifier | 2.349 | 0.1253 | 1.906 | 0.167 |
| He purifier vs.<br>He purifier + new support | 8.232 | **0.0041** | 9.246 | **0.002** |
| Baseline vs.<br>He purifier + new support | 11.799 | **0.0006** | 13.716 | **0.0002** |
| Density | | | | |
| | asymptotic | | M-SLRT | |
| | statistic | p-value | statistic | p-value |
| Baseline vs He purifier | 0.591 | 0.442 | 0.468 | 0.494 |
| He purifier vs<br>He purifier + new support | 0.190 | 0.663 | 0.193 | 0.660 |
| Baseline vs<br>He purifier + new support | 1.235 | 0.266 | 1.107 | 0.293 |

Results presented above show that when He purifier is installed, switching from the old support wafer to the new one results in a statistically significant increase in the height of the forest and a statistically significant decrease in the CV of height. Therefore, analysis of *in situ* growth kinetics is needed to understand the mechanism of the significant change in height and its CV, i.e., whether it results from an increase in growth rate or in catalytic lifetime. We use *in situ* videography collected during growth to plot growth kinetics using contrast adjusted image processing, as explained in our previous work [27]. As seen in Figure 8, results show that both cases have similar initial growth rates, suggesting that the average temperature is the same in both cases. Nevertheless, by comparing the case that has He purifier with the case that has both the He purifier and the new support, we see two major differences: (1) comparing the red curve to the black curve in Figure 8a, the red curve shows a faster rate of forest height increase during the later stages of growth before self-termination, as highlighted in the shaded area, and (2) the forest geometry is more uniform with a flat top surface in the case of using our new support, as shown in Figures 8b and 8c. This geometric nonuniformity may arise due to spatial variations of temperatures across the surface of the catalyst. Thus, these results demonstrate significant improvements achieved by using our redesigned substrate support on both geometry uniformity of CNT forests and run-to-run variations.

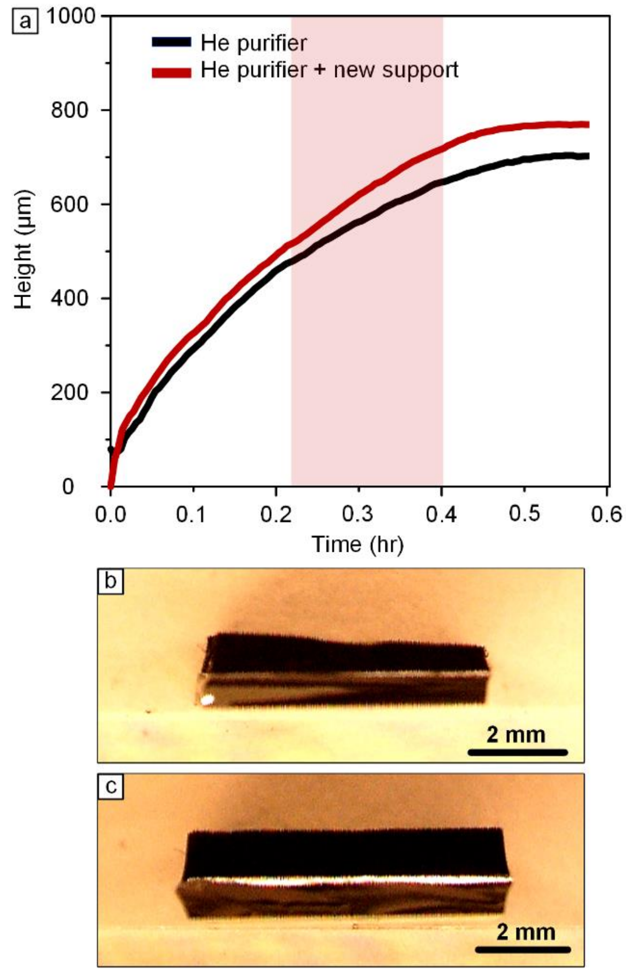


**Figure 8:** (a) Growth kinetics curves extracted from *in situ* videography for two cases: He purifier only shown in (b) and He purifier with new support wafer shown in (c).

## 4. CONCLUSION

Introducing new processing steps and/or parameters with the aim of improving reproducibility in the CVD growth of CNT forests requires statistical data analytics to decide what parameters lead to significant reduction in the variability of growth. Here we investigated the effects of two modifications to our growth setup, namely adding He purifier and new design for the support wafer, on growth consistency. He purifier was added to eliminate small uncontrolled variations of gaseous species in the reactor, while the new support wafer was designed with the aim of stabilizing the location of the substrate and creating a more uniform temperature profile across the substrate. When He purifier was installed, changing the support wafer from the old design to the new one led to statistically and practically significant improvement in forest height and its CV. In particular, a 17-fold reduction in variability of height and a 2-fold reduction in variability of density were achieved. Hence, our results demonstrate that our unique custom-designed reactor and process enable growing uniform CNT forests with less than 0.01 CV.

## ACKNOWLEDGEMENTS

This research was supported by the National Science Foundation (Award Number: 1825772) and the Department of Industrial Engineering at the University of Pittsburgh.

## REFERENCES

1. Bedewy, M., Meshot, E.R., Guo, H., Verploegen, E.A., Lu, W., Hart, A.J.J.: Collective mechanism for the evolution and self-termination of vertically aligned carbon nanotube growth. J. Phys. Chem. C. 113, 20576–20582 (2009). doi:10.1021/jp904152v
2. Bedewy, M., Meshot, E.R., Reinker, M.J., Hart, A.J.: Population growth dynamics of carbon nanotubes. ACS Nano. 5, 8974–8989 (2011). doi:10.1021/nn203144f
3. Bedewy, M., Viswanath, B., Meshot, E.R., Zakharov, D.N., Stach, E.A., Hart, A.J.: Measurement of the Dewetting, Nucleation, and Deactivation Kinetics of Carbon Nanotube Population Growth by Environmental Transmission Electron Microscopy. Chem. Mater. 28, 3804–3813 (2016). doi:10.1021/acs.chemmater.6b00798
4. Balakrishnan, V., Bedewy, M., Meshot, E.R., Pattinson, S.W., Polsen, E.S., Laye, F., Zakharov, D.N., Stach, E.A., Hart, A.J.: Real-Time Imaging of Self-Organization and Mechanical Competition in Carbon Nanotube Forest Growth. ACS Nano. 10, 11496–11504 (2016). doi:10.1021/acsnano.6b07251
5. Tong, T., Zhao, Y., Delzeit, L., Kashani, A., Meyyappan, M., Majumdar, A.: Dense Vertically Aligned Multiwalled Carbon Nanotube Arrays as Thermal Interface Materials. IEEE Trans. Components Packag. Technol. 30, 92–100 (2007). doi:10.1109/TCAPT.2007.892079
6. Majumder, M., Chopra, N., Andrews, R., Hinds, B.J.: Enhanced flow in carbon nanotubes. Nature. 438, 44–44 (2005). doi:10.1038/438044a
7. Wei, B.Q., Vajtai, R., Ajayan, P.M.: Reliability and current carrying capacity of carbon nanotubes. Appl. Phys. Lett. 79, 1172–1174 (2001). doi:10.1063/1.1396632
8. Pander, A., Hatta, A., Furuta, H.: Optimization of catalyst formation conditions for synthesis of carbon nanotubes using Taguchi method. Appl. Surf. Sci. 371, 425–435 (2016). doi:10.1016/j.apsusc.2016.02.216
9. In, J. Bin, Grigoropoulos, C.P., Chernov, A.A., Noy, A.: Hidden role of trace gas impurities in chemical vapor deposition growth of vertically-aligned carbon nanotube arrays. Appl. Phys. Lett. 98, 153102 (2011). doi:10.1063/1.3573830
10. In, J. Bin, Grigoropoulos, C.P., Chernov, A.A., Noy, A.: Growth kinetics of vertically aligned carbon nanotube arrays in clean oxygen-free conditions. ACS Nano. 5, 9602–9610 (2011). doi:10.1021/nn2028715
11. Oliver, C.R., Polsen, E.S., Meshot, E.R., Tawfick, S., Park, S.J., Bedewy, M., Hart, A.J.: Statistical analysis of variation in laboratory growth of carbon nanotube forests and recommendations for improved consistency. ACS Nano. 7, 3565–3580 (2013). doi:10.1021/nn400507y
12. Li, J., Bedewy, M., White, A.O., Polsen, E.S., Tawfick, S., John Hart, A.: Highly Consistent Atmospheric Pressure Synthesis of Carbon Nanotube Forests by Mitigation of Moisture Transients. J. Phys. Chem. C. 120, 11277−11287 (2016). doi:10.1021/acs.jpcc.6b02878
13. Shi, W., Li, J., Polsen, E.S., Oliver, C.R., Zhao, Y., Meshot, E.R., Barclay, M., Fairbrother, D.H., Hart, A.J., Plata, D.L.: Oxygen-promoted catalyst sintering influences number density, alignment, and wall number of vertically aligned carbon nanotubes. Nanoscale. 9, 5222–5233 (2017). doi:10.1039/c6nr09802a
14. Carpena-Núñez, J., Anibal Boscoboinik, J., Saber, S., Rao, R., Zhong, J.-Q., R. Maschmann, M., R. Kidambi, P., T. Dee, N., N. Zakharov, D., John Hart, A., A. Stach, E., Maruyama, B.: Isolating the Roles of Hydrogen Exposure and Trace Carbon Contamination on the Formation of Active Catalyst Populations for Carbon Nanotube Growth. ACS Nano. 13, 8736–8748 (2019). doi:10.1021/acsnano.9b01382
15. Dee, N.T., Li, J., White, A.O., Jacob, C., Shi, W., Kidambi, P.R., Cui, K., Zakharov, D.N., Janković, N.Z., Bedewy, M., Chazot, C.A.C., Carpena-Núñez, J., Maruyama, B., Stach, E.A., Plata, D.L., Hart, A.J.: Carbon-assisted catalyst pretreatment enables straightforward synthesis of high-density carbon nanotube forests. Carbon N. Y. (2019). doi:10.1016/J.CARBON.2019.06.083
16. Youn, S.K., Frouzakis, C.E., Gopi, B.P., Robertson, J., Teo, K.B.K., Park, H.G.: Temperature gradient chemical vapor deposition of vertically aligned carbon nanotubes. Carbon N. Y. 54, 343–352 (2013). doi:10.1016/j.carbon.2012.11.046
17. Yang, N., Youn, S.K., Frouzakis, C.E., Park, H.G.: An effect of gas-phase reactions on the vertically aligned CNT growth by temperature gradient chemical vapor deposition. Carbon N. Y. 130, 607–613 (2018). doi:10.1016/j.carbon.2018.01.072
18. Qi, H., Yuan, D., Liu, J.: Two-stage growth of single-walled carbon nanotubes. J. Phys. Chem. C. 111, 6158–6160 (2007). doi:10.1021/jp071448q
19. Amama, P.B., Pint, C.L., McJilton, L., Kim, S.M., Stach,

 

E. a, Murray, P.T., Hauge, R.H., Maruyama, B.: Role of Water in Super Growth of Single-Walled Carbon Nanotube Carpets. Nano Lett. 9, 44–49 (2009). doi:Doi 10.1021/Nl801876h

20. Lee, J., Abdulhafez, M., Bedewy, M.: Data Analytics Enables Significant Improvement of Robustness in Chemical Vapor Deposition of Carbon Nanotubes Based on Vacuum Baking. Ind. Eng. Chem. Res. 58, 11999–12009 (2019). doi:10.1021/acs.iecr.9b01725
21. Doering, R., Nishi, Y. eds: Handbook of Semiconductor manufacturing Technology. Taylor and Francis (2007)
22. Lee, J., Abdulhafez, M., Bedewy, M.: Multizone Rapid Thermal Processing to Overcome Challenges in Carbon Nanotube Manufacturing by Chemical Vapor Deposition. J. Manuf. Sci. Eng. 141, (2019). doi:10.1115/1.4044104
23. Lee, J., Abdulhafez, M., Bedewy, M.: Decoupling Catalyst Dewetting, Gas Decomposition, and Surface Reactions in Carbon Nanotube Forest Growth Reveals Dependence of Density on Nucleation Temperature. J. Phys. Chem. C. 123, 28726–28738 (2019). doi:10.1021/acs.jpcc.9b07894
24. Marwick, B., Krishnamoorthy, K.: cvequality: Tests for the Equality of Coefficients of Variation from Multiple Groups, R software package version 0.1.3.
25. Feltz, C.J., Miller, G.E.: An Asymptotic Test for the Equality of Coefficients of Variation from k Populations. Stat. Med. 15, 647–658 (1996). doi:10.1002/(SICI)1097-0258(19960330)15:6<647::AID-SIM184>3.0.CO;2-P
26. Krishnamoorthy, K., Lee, M.: Improved tests for the equality of normal coefficients of variation. Comput. Stat. 29, 215–232 (2014). doi:10.1007/s00180-013-0445-2
27. Abdulhafez, M., Lee, J., Bedewy, M.: In Situ Measurement of Carbon Nanotube Growth Kinetics in a Rapid Thermal Chemical Vapor Deposition Reactor With Multizone Infrared Heating. J. Micro Nano-Manufacturing. 8, (2020). doi:10.1115/1.4046033